Steady-State Kinetic Characterization of RB69 DNA Polymerase Mutants That Affect dNTP Incorporation†

Guangwei Yang,‡,§ T.-C. Lin,‡ J. Karam,|| and W. H. Konigsberg*,‡

Department of Molecular Biophysics and Biochemistry, Yale University, 333 Cedar Street, New Haven, Connecticut 06520, Department of Biochemistry and Molecular Biology, College of Life Science, Peking University, Beijing, 100871 PRC, and Department of Biochemistry SL-43, Tulane University School of Medicine, 1430 Tulane Avenue, New Orleans, Louisiana 70112

Received March 19, 1999; Revised Manuscript Received April 27, 1999

ABSTRACT: The function of six highly conserved residues (Arg482, Lys483, Lys486, Lys560, Asn564, and Tyr567) in the fingers domain of bacteriophage RB69 DNA polymerase (RB69 gp43) were analyzed by kinetic studies with mutants in which each of these residues was replaced with Ala. Our results suggest that Arg482, Lys486, Lys560, and Asn564 contact the incoming dNTP during the nucleotidyl transfer reaction as judged by variations in apparent K_m and k_{cat} values for dNTP incorporation by these mutants compared to those for the exonuclease deficient parental polymerase under steady-state conditions. On the basis of our studies, as well as on the basis of the crystal structure of RB69 gp43, we propose that a conformational change in the fingers domain, which presumably occurs prior to polymerization, brings the side chains of Arg482, Lys486, Lys560, and Asn564 into the vicinity of the primer−template terminus where they can contact the triphosphate moiety of the incoming dNTP. In particular, on the basis of structural studies reported for the "closed" forms of two other DNA polymerases and from the kinetic studies reported here, we suggest that (i) Lys560 and Asn564 contact the nonbonding oxygens of the α and β phosphates, respectively, and (ii) both Arg482 and Lys486 contact the γ phosphate oxygens of the incoming dNTP of RB69 gp43 prior to the nucleotidyl transfer reaction. We also found that Ala substitutions at each of these four RB69 gp43 sites could incorporate dGDP as a substrate, although with markedly reduced efficiency compared to that with dGTP. In contrast in the parental exo$^-$ background, the K483A and Y567A substituted enzymes could not use dGDP as a substrate for primer extension. These results, taken together, are consistent with the putative roles of the four conserved residues in RB69 gp43 as stated above.

The DNA replicase of bacteriophage T4 has proven to be a fruitful system for studying fundamental mechanisms of DNA replication that can be generalized to other DNA replicases. Many of the protein components of the T4 replicase share sequence similarities with proteins having corresponding functions in eukaryotic cells (for reviews, see refs *1*−*5*). Attempts to gain a deeper understanding of the structure−function relationship in the T4 system have been hampered by the failure to obtain useful crystals of T4 DNA polymerase (T4 gp43) despite intensive efforts. This situation changed dramatically with studies of the homologous polymerase from phage RB69, a phylogenetic relative of T4 (*6*, *7*). The primary structures of the DNA polymerases of T4 and RB69 share similar or identical residues at 74% of all positions and many similarities with the B family (pol[1] α-like) DNA polymerases found in eukaryotes (*6*, *8*, *9*). Many of the pol α-like DNA polymerases have a number of highly conserved regions with essentially invariant residues in a well-defined linear relationship to each other (*10*−*14*). With determination of the crystal structure of RB69 gp43 as the first representative of this class, it is now possible to place these conserved residues in a structural context (*9*, *15*). However, due to the absence of an incoming dNTP or ddNTP in the crystal structure, it has not been possible to define the dNTP binding pocket or identify residues that contact portions of the dNTP. Nevertheless, it is possible to make some inferences about the gp43 residues that are likely involved in these interactions on the basis of analogies with the crystal structures of the closed forms of T7 DNA polymerase (*16*) and Klentaq (*17*), which are complexed with a primer−template and a ddNTP. With this in mind, we have targeted six highly conserved residues in the fingers domain of RB69 gp43 for site-directed mutagenesis. Three of these

† This work was supported in part by NIH Grants GM54627 amd GM18842.

* To whom correspondence should be addressed: Department of Molecular Biophysics and Biochemistry, Yale University, 333 Cedar St., New Haven, CT 06520. Phone: (203) 785-4599. Fax: (203) 785-6404. E-mail: william.konigsberg@yale.edu.

‡ Yale University.

§ Peking University.

|| Tulane University School of Medicine.

[1] Abbreviations: dATP, deoxyadenosine triphosphate; dCTP, deoxycytosine triphosphate; dGTP, deoxyguanosine triphosphate; dTTP, deoxythymidine triphosphate; dUTP, deoxyuridine triphosphate; dNTP, deoxynucleoside triphosphate; dGDP, deoxyguanosine diphosphate; KF, Klenow fragment; Klentaq, Klenow fragment of the *Thermus aquaticus* DNA polymerase I; pol, polymerase; exo, 3′ to 5′ exonuclease; SDS−PAGE, sodium dodecyl sulfate−polyacrylamide gel electrophoresis; Tris, tris(hydroxymethyl)aminomethane; DTT, dithiothreitol; EDTA, ethylenediaminetetraacetic acid disodium salt; dsDNA, double-stranded DNA.

10.1021/bi990653w CCC: $18.00 © 1999 American Chemical Society
Published on Web 06/03/1999

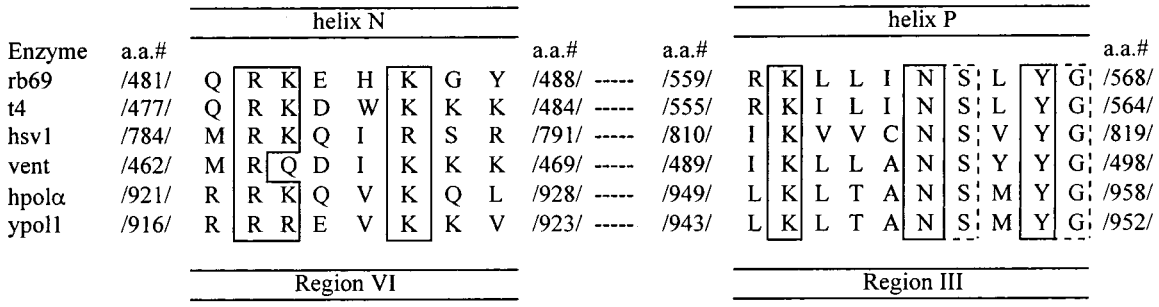

FIGURE 1: Sequence alignment in the fingers domain among pol α (B family) DNA polymerases (*9*). Amino acid residues 481−488 and 559−568 of RB69 gp43 were aligned with corresponding residues from five other DNA polymerases in the pol α family. Those shown are RB69 (rb69), T4 (t4), herpes simplex virus I (hsv1), human pol α (hpolα), and *Saccharomyces cerevisiae* pol I (ypol1). The six conserved residues that were replaced with Ala in RB69 are in solid boxes along with the identical residues from other polymerases. The two conserved residues that were not altered are enclosed in boxes with dashed lines. The first set of three conserved residues is in helix N (shown above) and in region VI (shown below). The second set of three conserved residues is in helix P (shown above) and in region III (shown below) (*40*).

residues (Arg482, Lys483, and Lys486) are in region VI, and the other three (Lys560, Asn564, and Tyr567) are in region III (see Figure 1) (9, *10*). Previous work from other laboratories has provided evidence that the $\underline{K}X_3\underline{N}S\underline{X}\underline{Y}G$ sequence in region III of polymerases from the B family (*13*, *18*−*22*) plays a role in binding incoming dNTPs and has a functional counterpart in the $\underline{K}X_4\underline{N}S\underline{X}\underline{Y}G$ sequence (motif B) in the O helix of pol I family polymerases as represented by Klenow fragment (KF) (*23*). Thus, we examined the potential role of the six conserved residues in regions III and VI of RB69 gp43 in dNTP binding and in the transition state during phosphodiester bond formation. We have replaced each of these residues with Ala and characterized the resulting mutants in terms of their steady-state kinetic parameters for dNTP incorporation. In addition, to determine if some of these conserved residues interact with the phosphate moiety of the incoming dNTP, we examined the ability of the gp43 mutants to incorporate dGDP and found that four mutants (R482A, K486A, K560A, and N564A) could use dGDP with low efficiency whereas the parental exo$^-$ enzyme (D222A/D327A) and the K483A and Y567A mutants could not. Taken together with the kinetic parameters, these results suggest that the four conserved basic residues could make contact with the phosphate portion of the incoming dNTP during the primer extension reaction.

EXPERIMENTAL PROCEDURES

Materials

The sources of reagents were as follows. Restriction endonucleases and T4 polynucleotide kinase were obtained from New England Biolabs. dGDP was from Sigma and [γ-^{32}P]ATP from Amersham Corp. The QuickChange Site-Directed Mutagenesis Kit and *Escherichia coli* strain BL21/DE3 were from Stratagene. dNTPs were from Pharmacia/LKB. Chromatography media were from either Pharmacia or Bio-Rad and electrophoresis reagents from American Bioanalytical Corp., and the Complete protease inhibitor tablet was from Boehringer-Mannheim. Plasmid CW50 (pCW50) was constructed by C. C. Wang in the laboratory of J. Karam (Tulane University), and oligonucleotides and DNA sequencing services were provided by the W. M. Keck Foundation Biotechnology Resource Laboratory (Yale University). All other chemicals used were of analytical grade.

Methods

Oligonucleotide-Directed Mutagenesis. Two plasmids, pCW50 and pCJ42H, which express high levels of RB69 gp43 were used for site-directed mutagenesis. Both plasmids were constructed by inserting the gene for RB69 gp43 exo deficient (D222A/D327A) into the *Bam*HI and *Hin*dIII sites of the expression vector pSP72 (Promega Corp.). The resulting plasmid expressed the parental exo$^-$ enzyme. The only difference between pCW50 and pCJ42H was that pCJ42H contained a DNA sequence encoding three His residues at the 3′-terminus (3′-His tag) of the polymerase gene. The specific polymerase (pol) and exonuclease (exo) activities of the gp43 with the $(His)_3$ tag were identical to the parental exo$^-$ gp43 (data not shown).

We followed the PCR-based protocol of the QuickChange Site-Directed Mutagenesis Kit to obtain the desired mutations. The presence of the altered codon was confirmed by DNA sequencing.

Expression and Purification of RB69 gp43 and Its Mutant Derivatives. Expression of wild-type and mutant RB69 gp43 was carried out essentially as described previously (*24*). Purification of plasmid-encoded gp43 lacking the $(His)_3$ tag utilized about 3 g of cells that were lysed in 50 mL of lysis buffer [50 mM Tris-HCl (pH 8.0), 1 mM EDTA, and 10 mM DTT, containing one Complete protease inhibitor tablet]. After sonication on ice for eight 30 s cycles, the lysates were cleared by centrifugation at 180000*g* for 60 min and the supernatants dialyzed overnight at 4 °C against 2 L of dialysis buffer [40 mM Tris-HCl (pH 7.5), 1 mM EDTA, 10% glycerol, and 10 mM β-mercaptoethanol]. The dialysate was loaded onto the DEAE Sepharose fast flow column (50 cm × 3 cm) which had been equilibrated with buffer A (30 mM Tris-HCl, 1 mM EDTA, 1 mM DTT, 1 mM $Na_2S_2O_5$, 0.1% NaN_3, and 10% glycerol). After the column had been washed with 450 mL of buffer A containing 100 mM KCl, bound material was eluted using 200 mL of buffer A containing 200 mM KCl. Fractions containing gp43 (as judged by SDS−PAGE) were pooled and applied directly to the Source 30Q column (10 cm × 2 cm) which had been equilibrated with buffer A. After the column had been washed with 150 mL of 100 mM KCl in buffer A, fractions containing gp43 were eluted with 100 mL of 200 mM KCl in buffer A. These fractions were pooled, dialyzed overnight at 4 °C against

Table 1: Oligonucleotides for Determination of Kinetic Parameters for dNTP Incorporation

Primer /template	dNTP(s) substrate	Sequence[a,b]	
13/20TG	dATP	5′ - CCG ACC AGC CTT G - 3′ 3′ - GGC TGG TCG GAA C**T**G GGG GG - 5′	13mer 20mer
13/20GT	dCTP	5′ - CCG ACC AGC CTT G - 3′ 3′ - GGC TGG TCG GAA C**G**T TTT TT - 5′	13mer 20mer
13/20CA	dGTP	5′ - CCG ACC ACG GAA C - 3′ 3′ - GGC TGG TGC CTT G**C**A AAA AA - 5′	13mer 20mer
13/20AC	dTTP &dUTP	5′ - CCG ACC ACG GAA C - 3′ 3′ - GGC TGG TGC CTT G**A**C CCC CC - 5′	13mer 20mer

[a] The nucleotide residues in the template are complementary to the incoming dNTPs and, for which kinetic parameters were determined, are boldface and underlined. [b] The 13mer primers were 5′-^{32}P-labeled and then annealed with the 20mer templates.

1 L of buffer B (25 mM K_2HPO_4, 25 mM KH_2PO_4, 1 mM DTT, 1 mM $Na_2S_2O_5$, 0.1% NaN_3, and 10% glycerol), and then applied to the ceramic hydroxyapatite type I column (60 cm × 2 cm) which had been equilibrated with buffer B. After the column had been washed with 150 mL of a solution containing 95% buffer B and 5% buffer C (200 mM K_2HPO_4, 200 mM KH_2PO_4, 1 mM DTT, 1 mM $Na_2S_2O_5$, 0.1% NaN_3, and 10% glycerol) and 150 mL of a solution containing 90% buffer B and 10% buffer C, the highly purified RB69 gp43 was eluted with 150 mL of buffer C. Fractions containing gp43 were pooled, dialyzed overnight at 4 °C against 2 L of protein storage buffer [20 mM Tris-HCl (pH 7.5), 0.1 mM EDTA, 5 mM β-mercaptoethanol, and 50% glycerol] and then concentrated 5-fold by pressure filtration to a final concentration of about 10 mg/mL.

Purification of gp43 with the (His)$_3$ Tag. After lysis sonication and centrifugation as described above, the supernatant was dialyzed against dialysis buffer, and the gp43 purified using a chelating Sepharose fast flow column (2.5 cm × 1.0 cm) according to the protocol provided by Pharmacia. The eluted fractions were pooled, dialyzed against dialysis buffer, and loaded onto a MonoQ column (5 cm × 0.75 cm) which had been equilibrated with buffer A. After the column had been washed once with 25 mL of buffer A, the fractions containing the RB69 gp43 with the $(His)_3$ tag were eluted with 90 mL of a linear gradient made from buffer A and buffer A containing 2 M KCl.

The purity of gp43 preparations was judged by SDS−PAGE, and the enzyme concentrations were determined spectrophotometrically as described previously (*25*).

Exonuclease Assays. Assays for 3′ to 5′ exonuclease activity on a 16/24mer double-stranded DNA substrate were carried out as described previously (*24*, *25*), except that the oligonucleotide concentration was 50 nM instead of 600 nM in the experiments reported here.

Preparation of a 13/20mer for Primer Extension Assays. The exo$^-$ RB69 gp43 and its derivatives still exhibited residual exonuclease activity (but reduced by 10^4-fold as compared to that of the wild type) (*25*), and it was necessary to design substrates that would allow estimation of the rates of a single nucleotide addition without interference from this competing activity. Substrate design was especially important for mutants that had very low pol activity. For this purpose, four sets of 13/20mer dsDNA primer−templates were constructed in which the first base distal to the 3′-primer terminus on the template strand was complementary to the incoming dNTP for which kinetic parameters were to be estimated (Table 1). The remaining six bases in the template were identical to each other but different from the first. The concentration of the first incoming dNTP was varied, but the concentration of the dNTP complementary to the next six template bases was never more than 1 mM and was always 100-fold greater than the concentration of the dNTP being studied. Under these conditions, the primer was extended to a 20mer very rapidly once the limiting dNTP reacted with the 3′-hydroxyl at the primer terminus. As a result, very little of the fully extended primer was degraded by the residual exo activity of the mutant gp43s. The 13mers were 5′-labeled with γ-^{32}P by standard procedures, annealed with the complementary 20mers, and used as substrates for primer extension assays.

Primer Extension Assays and Kinetic Analyses. The 10 μL reaction mixture for primer extension assays contained the appropriate 13/20mer at 50 nM, 66 mM Tris-HCl (pH 8.8), 17 mM $(NH_4)_2SO_4$, 10 mM β-mercaptoethanol, 6.5 mM $MgSO_4$, 10% glycerol, 166 μg/mL BSA, various concentrations of the first incoming dNTP, a 100-fold excess of the dNTP complementary to the remaining bases on the template strand, and various concentrations of the parental exo$^-$ or mutant RB69 gp43 preparations. Assays and kinetic analyses were performed as described previously (*24*, *25*). For each K_m and k_{cat} determination, we used five different concentrations of the first incoming dNTP (which spanned a 10-fold range on either side of the K_m), and a large excess of the dNTP complementary to the remaining six bases on the template. Values obtained for the enzyme concentration required to yield a 50% depletion of the primer (involving elongation of the 13mer at a fixed time) were used to estimate the velocity of the reaction. The data obtained from at least three assays where the derivation from linearity was less than

Table 2: Steady-State Kinetic Parameters for Incorporation of dATP, dCTP, dGTP, dTTP, and dUTP

	dATP		dCTP		dGTP		dTTP		dUTP	
enzyme[a]	K_m (μM)	k_{cat} (s^{-1})	K_m (μM)	k_{cat} (s^{-1})	K_m (μM)	k_{cat} (s^{-1})	K_m (μM)	k_{cat} (s^{-1})	K_m (μM)	k_{cat} (s^{-1})
parental exo$^-$	0.34	0.22	0.57	1.0	0.17	0.37	2.4	0.57	1.3	0.78
K483A	0.33	0.23	0.53	0.48	0.37	0.47	4.2	0.50	2.3	0.33
Y567A	0.59	0.06	0.42	0.15	0.20	0.62	4.0	1.3	2.4	1.0
R482A	6.4	5.3×10^{-3}	15	3.4×10^{-2}	5.1	5.3×10^{-3}	5.2	1.8×10^{-3}	2.7	1.1×10^{-3}
K486A	6.0	6.0×10^{-3}	17	9.3×10^{-2}	6.6	1.9×10^{-3}	5.8	4.4×10^{-4}	2.2	2.2×10^{-4}
K560A	1.0×10^2	0.20	19	6.5×10^{-2}	51	0.17	3.3×10^3	2.1	3.8×10^2	0.30
N564A	10	8.3×10^{-2}	6.3	0.16	1.7	0.18	64	0.42	25	0.33

[a] All the enzymes in this study carry the D222A/D327A double mutation which makes them deficient in 3′ to 5′ exonuclease activity.

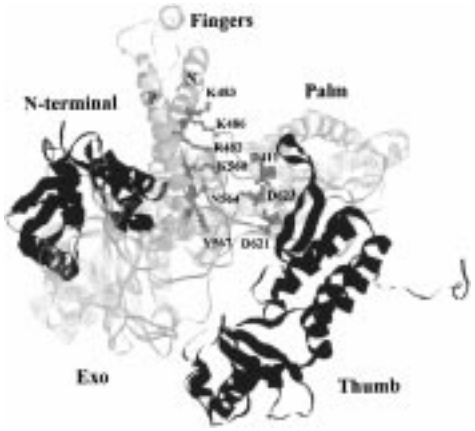

FIGURE 2: Ribbon diagram of RB69 DNA polymerase from Wang et al. (*9*) showing the relative location of the five domains (Exo, N-terminal, Fingers, Palm, and Thumb), each denoted by a different shading. The relative locations of the six highly conserved residues that were altered in the fingers domain are also shown as are the two conserved Asp residues (Asp411 and Asp623) in the palm domain.

50% were averaged and reported. Kinetic data were analyzed by Lineweaver−Burk double-reciprocal plots.

dGDP Purification and dGDP Incorporation Assays. We used the double-stranded oligomer 13/20CC shown below together with the parental exo$^-$ polymerase to remove contaminating dGTP in commercial dGDP: 5′-CCG ACC ACG GAA C-3′ (13mer) and 3′-GGC TGG TGC CTT GCC CCC CC-5′ (20mer) (13/20CC). The 1 mL reaction mixture contained the 13/20CC oligomer at 50 μM, 1 mM commercial dGDP, 267 nM RB69 gp43 parental exo$^-$ mutant (D222A/D327A), 66 mM Tris-HCl (pH 8.8), 17 mM $(NH_4)_2SO_4$, 10 mM β-mercaptoethanol, 6.5 mM $MgSO_4$, 10% glycerol, and 166 μg/mL BSA. After incubation at 30 °C for 1 h, the reaction was stopped by heating the mixture to 75 °C for 10 min to inactivate gp43 and then passed over a Sephadex G-10 column to separate dGDP from the dsDNA primer−template and the denatured enzyme. Before the recovered dGDP was used as a substrate in the primer extension assay, its purity was checked for lack of incorporation in primer extension assays with the parental exo$^-$ enzyme and the 13/20CC primer−template. The assays for determining the kinetic parameters for dGDP incorporation were the same as described above for the primer extension assays with dGTP.

RESULTS

Site-Directed Mutagenesis and the Preparation of Mutant Polymerases. To identify amino acid residues in RB69 gp43 that may contribute to dNTP binding or participate in the nucleotidyl transfer reaction, we first examined the aligned sequences of B family DNA polymerases shown in Figure 1 (*9*, *14*). We note six highly conserved residues in the fingers domain of gp43: Arg482, Lys483, and Lys486 located in helix N and Lys560, Asn564, and Tyr567 located in helix P (Figures 1 and 2) (*9*). We constructed gp43 mutants in which these residues were replaced by Ala and used them for steady-state kinetic studies designed to test their ability to utilize each of the four dNTPs and dUTP in extending a 13mer primer annealed to a complementary template with a seven-residue 5′-overhang (Table 1).

Because we anticipated that some of the mutants would have greatly diminished polymerase activity, it was essential to cripple the 3′ to 5′ exo function of the enzyme as thoroughly as possible so that measurements of primer extension rates would not be affected by turnover of the 3′-terminal nucleotide. For this reason, we employed a plasmid that specifies the exo deficient D222A/D327A RB69 gp43 as the starting point for construction of the six gp43 mutants (*25*; C. C. Wang, unpublished results). By using PCR with appropriate primers, we constructed a set of mutants in which Ala replaced each of the designated residues in the parental exo$^-$ background. After transformation, cells harboring the mutant plasmids were induced and the mutant polymerases were isolated and purified to homogeneity as described in Experimental Procedures.

Steady-State Kinetic Parameters for dNTP Incorporation with the Parental Exo$^-$ Polymerase. Primer extension assays showed that four of the exo$^-$ gp43 mutants (R482A, K486A, K560A, and N564A) had reduced pol activity (data not shown). To better understand the basis for this reduction, we estimated steady-state kinetic parameters for the parental exo$^-$ enzyme and for its four mutant derivatives described above with respect to incorporation of each of the four dNTPs and dUTP (Table 2).

The steady-state K_m values[2] for incorporation of different dNTPs by the parental exo$^-$ enzyme showed that $K_{m(dTTP)}$ was about 15-fold greater than $K_{m(dGTP)}$ which had the lowest value (0.17 μM) (Table 2). The K_m values for dCTP and dATP were slightly higher than that for dGTP (Table 2). The k_{cat} values[2] also differed from one another, i.e., $k_{cat\ (dCTP)}$ being almost 5-fold higher than $k_{cat(dATP)}$. The kinetic parameters for dUTP incorporation by the parental exo$^-$ enzyme are almost the same as for dTTP, indicating that the absence of a 5′-methyl group on the pyrimidine ring does not significantly affect the rate of this reaction.

[2] For simplicity, all the K_m and k_{cat} values refer to apparent steady-state K_m and k_{cat} values.

Table 3: Steady-State Kinetic Parameters for Incorporation of dGTP and dGDP

	dGTP		dGDP	
enzyme[a]	K_m (μM)	k_{cat} (s^{-1})	K_m (μM)	k_{cat} (s^{-1})
parental exo$^-$	0.17	0.37	*b*	*b*
K483A	0.37	0.47	*b*	*b*
Y567A	0.20	0.62	*b*	*b*
R482A	5.1	5.3×10^{-3}	1.7	3.2×10^{-4}
K486A	6.6	1.9×10^{-3}	2.2	1.4×10^{-4}
K560A	51	0.17	3.0	7.8×10^{-5}
N564A	1.7	0.18	0.83	2.7×10^{-4}

[a] All the enzymes in this study carry the D222A/D327A double mutation and are therefore deficient in 3′ to 5′ exonuclease activity. [b] dGDP incorporation was undetectable under the same assay conditions used for R482A, K486A, K560A, and N564A.

Steady-State Kinetic Parameters for dNTP Incorporation with the Mutant Polymerases. Among the three mutations in helix N, one (K483A) had no effect on the kinetic parameters for incorporation of any of the dNTPs relative to the parental exo$^-$ enzyme. In contrast, R482A and K486A exhibited somewhat higher K_m values (2−40-fold) that depended on the dNTP being incorporated. The k_{cat} values estimated for these two mutants were dramatically decreased relative to the parental exo$^-$ enzyme: 30−700-fold for R482A and 10−3000-fold for K486A (the actual values varying with the dNTP substrate; see Table 2).

Among the three mutations in helix P, Y567A had kinetic parameters for dNTP incorporation nearly identical to those of the parental exo$^-$ enzyme. In contrast, K560A had much higher K_m values (40−300-fold) compared to those of the parental exo$^-$ polymerase, while the k_{cat} values decreased within a 4-fold range for all the dNTPs except $k_{cat(dCTP)}$, which was 20-fold lower than that of the parental exo$^-$ enzyme. Similarly, the N564A mutation in helix P also yielded higher K_m (10−30-fold) and lower k_{cat} (2−6-fold) values compared to the parental exo$^-$ enzyme.

Overall, the main effect of two of the mutations in helix N, R482A and K486A, was reduced k_{cat} values for dNTP incorporation, while the main effect of two of the mutations in helix P, K560A and N564A, was increased K_m values relative to those of the parental exo$^-$ enzyme.

Kinetic Parameters for dGDP Incorporation. Since all of the conserved residues targeted for replacement in the fingers domain have either positively charged or polar side chains, they have the potential to interact with the oxygen atoms of the triphosphate portion of the dNTPs. Because we knew that the parental exo$^-$ enzyme could not incorporate dGDP, we decided to investigate if any of the mutants in which charged or polar groups had been eliminated could use dNDP as a substrate for primer extension. Four mutants (R482A, K486A, K560A, and N564A) that exhibited large reductions in the efficiency of dGTP incorporation (k_{cat}/K_m, Table 3) were able to incorporate dGDP, while K483A, Y567A, and the parental exo$^-$ enzyme could not. A representative radioautograph that was used to demonstrate dGDP incorporation is shown in Figure 3 where the K560A mutant is compared to the parental enzyme. With the parental enzyme, dTTP can be misincorporated opposite C at high enzyme concentrations (between 8.9 and 89 nM) in the absence of dGDP (Figure 3, lanes 4 and 5). When dGDP is present, there is no further extension beyond the 14mer because

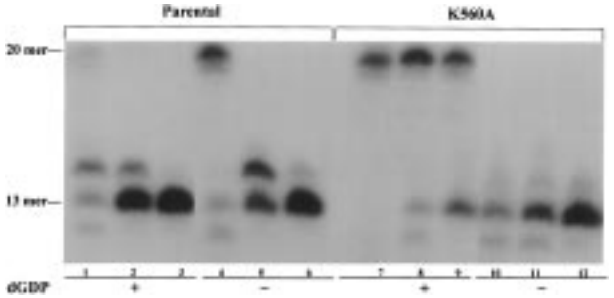

FIGURE 3: Autoradiograms showing the results of assays for dGDP incorporation by the parental exo$^-$ polymerase and its K560A mutant derivative. The reaction mixture contained 30 μM 13/20CA as primer−template (with the primer labeled with ^{32}P at the 5′-end, Table 1) and 100 μM dTTP. The reaction mixtures which included 30 μM purified dGDP were run in lanes 1−3 and 7−9, as indicated by the plus sign below the lane numbers. There was no dGDP in the reaction mixtures run in lanes 4−6 and 10−12 as indicated by the minus sign below the lane numbers. The enzyme concentrations for the parental enzyme were 89 nM (lanes 1 and 4), 8.9 nM (lanes 2 and 5), and 0.89 nM (lanes 3 and 6), and the concentrations for gp43 K560A were 16 μM (lanes 7 and 10), 1.6 μM (lanes 8 and 11), and 0.16 μM (lanes 9 and 12). The reactions were stopped by adding 0.1 M EDTA after incubating at 30 °C for 10 min. The mixtures were then analyzed by electrophoresis on 20% polyacrylamide gels containing 50% urea in TBE buffer.

dGDP inhibits the reaction (G. Yang, unpublished results) and the residual exo activity predominates (lanes 1 and 2). With the K560A mutant, dGDP is incorporated and the large molar excess of dTTP rapidly extends the primer to its full length (lanes 7−9). In the absence of dGDP, there is a small amount of misincorporation with this mutant, but the residual exo activity is sufficient to compete with further extension (lanes 10−12). Compared to the values obtained with dGTP, both the K_m and k_{cat} for dGDP incorporation decreased slightly with the R482A and K486A mutants. With the K560A and N564A mutants, the K_m values were only slightly reduced, whereas the k_{cat} values decreased dramatically (Table 3). Interestingly, the kinetic parameters for all four mutants, which were capable of incorporating dGDP, fell into a very narrow range, ~1 μM for K_m and ~10^{-4} s^{-1} for k_{cat}.

Specific Exonuclease Activities for the Mutant Polymerases. Because many of the mutants had low specific activities for polymerization, especially when dGDP was used as substrate, accurate estimation of K_m and k_{cat} values required that we determine the specific exo activities of each mutant so that the pol activity could be normalized correctly to that of the parental exo$^-$ enzyme. All the mutants, except for R482A (which behaves like the parental exo$^-$ polymerase), exhibited reduced residual exo activities on dsDNA as compared to the parent. For example, K483A, K486A, K560A, N564A, and Y567A have 12, 12, 10, 30, and 10% of the parental residual exo activity, respectively. These results are not surprising in view of the previously reported effects of mutations in the pol domain which have been shown to reduce the exo activity (*25*).

DISCUSSION

Kinetic Parameters for Incorporation of dNTPs by the Parental Exo$^-$ Polymerase. The relative K_m and k_{cat} values that we determined for dNTP incorporation with RB69 gp43 are different for each dNTP; it is tempting to think that these

differences mainly reflect the ability of the polymerase to discriminate among dNTPs because of complementarity between the incoming dNTP and the corresponding base on the template, but there may be other reasons as well. Although there are some pre-steady-state kinetic data available for the binding and reaction rates of all four dNTPs with Klentaq (*26*), the results are not directly comparable to the steady-state kinetic parameters reported here. The results reported by Astatke et al. (*27*) for incorporation of dGTP and dTTP by KF showed different K_m and k_{cat} values which were attributed to differences in the relative strengths of A·T versus G·C pairing of the incoming dNTP with its cognate base on the template. While this explanation may be valid for KF, it does not apply to the parental exo$^-$ form of RB69 gp43 studied here since $K_{m(dATP)}$ was nearly 7-fold lower than $K_{m(dTTP)}$, and $K_{m(dATP)}$ was also lower than $K_{m(dCTP)}$ (Table 2).

Residues That Interact with dNTPs and Affect Their Rates of Incorporation. Results obtained from crystal structures (*16*, *17*, *28*) and kinetic studies (*22*, *27*, *29*) suggest that the fingers domain of DNA polymerases are involved in dNTP binding, although the structural details of these domains differ among the individual enzymes (*30*, *31*).

The crystal structures of the closed form of the T7 DNA polymerase ternary complex (T7) (*16*) and the closed form of the Klentaq DNA polymerase ternary complex (Klentaq) (*17*) showed the incoming ddNTP bound in a pocket consisting of residues from the palm, thumb, and fingers domain of the DNA polymerase as well as part of the template strand just distal to the primer terminus. At least three highly conserved, positively charged, or polar residues located in the fingers domain contact the negatively charged triphosphate moiety through interactions with nonbonding oxygen atoms that are not coordinated to the divalent metal ions. For example, Arg518 (in T7) and Arg659 (in Klentaq) from helix O make contact with two oxygen atoms of the γ phosphate. His506 (in T7) and His639 (in Klentaq) from helix N contact the nonbonding oxygen of the β phosphate, and Lys522 (in T7) and Lys663 (in Klentaq) from helix O contact the oxygen of the α phosphate. These observations are consistent with kinetic studies on the corresponding residues Arg754, His734, and Lys758 in KF (*27*, *29*).

Our results show that mutants in which four highly conserved residues in helix N (Arg482 and Lys486) and helix P (Lys560 and Asn564) of the fingers domain of RB69 gp43 were replaced with Ala exhibit either increased K_m or decreased k_{cat} values for dNTP incorporation compared to those of the parental enzyme. Viewed in the context of structural data from the T7 and Klentaq polymerases, it seems reasonable to suggest that these residues in gp43 would be involved in dNTP binding. The RB69 gp43 crystal structure (Figure 2) (*9*) also shows that these four residues, in either the N or P helix, face the pol site, with their side chains pointing toward the pol catalytic center in the palm domain where three conserved acidic residues (Asp411, Asp621, and Asp623) are located (Figure 2). Two of these residues (Asp411 and Asp623), together with the incoming dNTP, would be expected to coordinate the two divalent metal ions required for catalysis (*16*, *30*−*35*). The location of the four conserved residues in the fingers makes it possible for their side chains to contact the phosphate moiety of incoming dNTP, providing that a conformational change occurs to bring helices N and P closer to the reaction center.

Mutants in which the other two conserved residues in the fingers domain (i.e., Lys483 and Tyr567) were replaced with Ala had almost no effect on the kinetic parameters as compared to the parental polymerase. In the gp43 crystal structure (Figure 2) (*9*), Lys483 is on the side of helix N pointing ~90° away from the catalytic site, and thus is unlikely to contact the incoming dNTP. We also found that the Y567A mutant incorporated mispaired dNTPs more efficiently than the parental polymerase (G. Yang, unpublished results), suggesting that Tyr567 has a role in maintaining fidelity, possibly by interacting with the base of the dNTP. There are examples in other DNA polymerases where single amino acid substitutions alter fidelity, e.g., Tyr766 in helix O of the fingers domain of KF (*36*, *37*) and Arg283 in the thumb domain of eukaryotic DNA polymerase β (*38*).

Kinetic studies with human polymerase α (*22*) and ϕ29 DNA polymerase (*39*) point to Lys950 in pol α and the corresponding Lys383 in ϕ29 (which are both equivalent to Lys560 in RB69 gp43) as having a role in dNTP binding. Specifically, Dong et al. (*22*) suggested that Lys950 in pol α interacts either directly or indirectly with one of the nonbonding oxygens of the α phosphate.

A Conformational Change May Involve the Fingers Domain of RB69 DNA Polymerase when a Ternary Complex Is Formed. From structural studies of DNA polymerases other than gp43, it appears that the presence of a primer−template and a correctly matched dNTP causes movement of the fingers domain toward the catalytic center by about 40°. Under such conditions, the polymerase shifts from an open to a closed conformation (*16*, *17*, *28*). In the case of Klentaq, a member of the pol I family, Li et al. (*17*, *28*) proposed that the incoming dNTP binds first to the positively charged and polar residues in the O helix prior to the conformational change. Once bound, the O helix rotates 46° to deliver the dNTP to the active site.

In the pol α family, there are no published reports of binary or ternary complexes. While the proposal by Li et al. (*17*, *28*) for Klentaq could apply to members of the pol α family, an alternative model may have to be considered as described below.

In the crystal structure of RB69 gp43 (*9*), the distances from the side chains of the four conserved residues in the fingers domain to the three conserved acidic residues in the palm domain range from 14 to 23 Å, i.e., greater than the distances between the nonbonding oxygens of dNTP (Figure 4B). Without a conformational change, it would not be possible for all four of the conserved residues in the fingers domain and the carboxylate ligands in the palm domain to simultaneously contact the triphosphate moiety of the incoming dNTP. On the basis of these considerations, we suggest that during polymerization, the fingers domain of RB69 gp43 moves toward the catalytic center, allowing all the residues at positions 482, 486, 560, and 564 to contact the incoming dNTP. Furthermore, we propose that the relative positions of helix P and N would also have to be slightly adjusted. Before adjustment, the four residues in the fingers domain would be too far apart from each other in the open conformation for all of them to contact the triphosphate moiety at the same time (Figure 4A). After adjustment, they could be reoriented to fit the shape of the triphosphate portion of the incoming dNTP (Figure 4A,B).

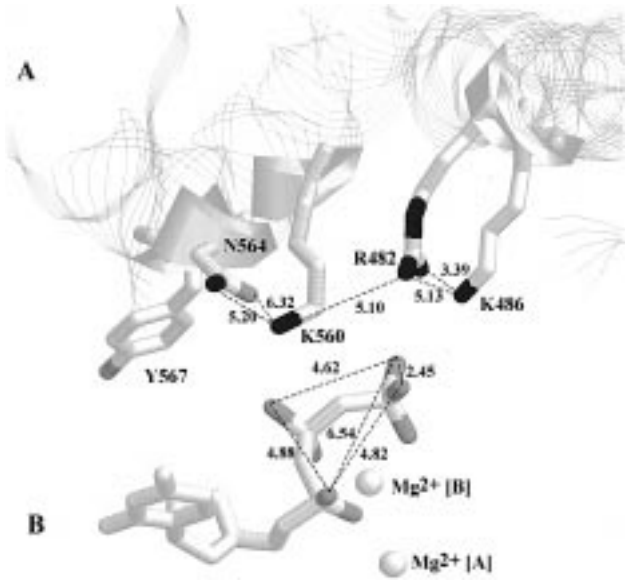

FIGURE 4: (A) Relative locations of the side chains of the six highly conserved residues in the fingers domain showing distances (in angstroms) between the nitrogen atoms at the end of the side chains. Also shown is the distance (6.32 Å) between the ϵ amino nitrogen of Lys560 and the β carbonyl oxygen of Asn564 (*9*). (B) Relative location of the nonbonding oxygen atoms of the phosphate moiety of dNTP and their distances from each other (in angstroms). Also indicated are the relative positions of the Mg^{2+} ions in the A and B sites [taken from the ternary structure of Klentaq (*17*)]. We present these depictions together to illustrate that a fit is possible between the triphosphate moiety and the side chains after the conformational change has been completed.

Proposed Interactions between the Fingers and the Phosphate Moiety of dNTP. If we accept the validity of sequence similarities between human pol α and RB69 gp43, and the suggested role of Lys950 in human pol α, it seems likely that the equivalent residue in RB69 gp43 (Lys560) would have the same function. On the basis of this tentative assignment, and taking into consideration the relative locations of Lys560, Asn564, Arg482, and Lys486 (Figures 2 and 4A) and the configuration of dNTP (Figure 4B), we propose that (i) Asn564 contacts the oxygen of β phosphate[3] and (ii) Arg482 and Lys486 contact two of the nonbonding γ phosphate oxygens.

All four mutants in the fingers domain differ in kinetic parameters from the parental enzyme (Table 2). The K_m values for gp43 K560A increased dramatically, but the k_{cat} values were almost unchanged; N564A also exhibited increased K_m values with almost unchanged k_{cat} values. In contrast, R482A and K486A had much lower k_{cat} values but only slightly increased K_m values. We suggest that if the interactions with the γ phosphate oxygens by Arg482 and Lys486 occur, they may assist in the removal of the pyrophosphate leaving group during the nucleotidyl transfer reaction so that loss of either Arg482 or Lys486 would be expected to decrease the rate of the chemical step. If Lys560 interacts with the α phosphate, instead of the leaving group, then it is not surprising that K560A has little effect on the k_{cat}. If Asn564 interacts with the oxygen of the β phosphate via H bonding rather than via the stronger ionic interactions that probably occur with the other positively charged residues, we would anticipate that the effect of the N564A mutant on the two kinetic parameters would be smaller than that exhibited by mutations in which positively charged residues have been changed to Ala. Our observations indicate that this is indeed the case.

dGDP Can Serve as a Substrate for Primer Extension with Certain Mutants. As shown in Table 3, the R482A, K486A, K560A, and N564A mutants were able to utilize dGDP as a substrate for primer extension. As far as we know, this is the first reported example of dNDP incorporation by any DNA polymerase (or mutant derivatives). The fact that K483A, Y567A, and the parental enzyme did not use dGDP rules out the possibility that the observed effects were due to a small amount of dGTP contaminating the dGDP used in the reaction. We should emphasize, however, that we cannot yet explain why these mutants are capable of incorporating dGDP. Among the difficulties in interpreting these results are (i) the inability of the parental enzyme to utilize dGDP (thus failing to provide a control for the kinetic data obtained with the mutants that do incorporate dGDP) and (ii) since the leaving group is a monophosphate rather than a pyrophosphate, the rate of the chemical step may be expected to change. In fact, we do observe that the k_{cat} is severely reduced with the mutants capable of using dGDP, but we are uncertain if the effect is due to the presence of a different leaving group. Nevertheless, the fact that only R482A, K486A, K560A, and N564A were able to utilize dGDP is intriguing since these four residues in the wild-type gp43 are those proposed in this paper to interact with the phosphate moiety of the incoming dNTP. Structural studies on ternary complexes of the mutant proteins would elucidate the spatial relationships between these residues and the incoming nucleoside triphosphate. Also, determination of pre-steady-state kinetic parameters would provide additional information about certain aspects of the mechanism, such as the rate-limiting step in the primer extension reaction catalyzed by these mutant polymerases.

While this paper was being reviewed, a report appeared (*41*) describing the crystal structure of a thermostable type B DNA polymerase which was compared with RB69 gp43 and found to have numerous structural similarities.

[3] As mentioned in the previous section, His residues that are uncharged at pH 8 contact the oxygen of the β phosphate in pol I family polymerases. Similarly, a polar uncharged residue, Asn564, is proposed to make the corresponding contact in RB69 gp43.

ACKNOWLEDGMENT

We thank J. Wang for helpful discussions.

REFERENCES

1. Baker, T. A., and Bell, S. P. (1998) *Cell 92*, 295−305.
2. Stillman, B. (1994) *Cell 78*, 725−8.
3. Tsurimoto, T., and Stillman, B. (1990) *Proc. Natl. Acad. Sci. U.S.A. 87*, 1023−7.
4. Tinker, R. L., Kassavetis, G. A., and Geiduschek, E. P. (1994) *EMBO J. 13*, 5330−7.
5. O'Donnell, M., Onrust, R., Dean, F. B., Chen, M., and Hurwitz, J. (1993) *Nucleic Acids Res. 21*, 1−3.
6. Wang, C. C., Yeh, L. S., and Karam, J. D. (1995) *J. Biol. Chem. 270*, 26558−64.
7. Yeh, L. S., Hsu, T., and Karam, J. D. (1998) *J. Bacteriol. 180*, 2005−13.
8. Braithwaite, D. K., and Ito, J. (1993) *Nucleic Acids Res. 21*, 787−802.
9. Wang, J., Sattar, A. K., Wang, C. C., Karam, J. D., Konigsberg, W. H., and Steitz, T. A. (1997) *Cell 89*, 1087−99.

10. Wang, T. S., Wong, S. W., and Korn, D. (1989) *FASEB J. 3*, 14−21.
11. Morrison, A., Bell, J. B., Kunkel, T. A., and Sugino, A. (1991) *Proc. Natl. Acad. Sci. U.S.A. 88*, 9473−7.
12. Blanco, L., Bernad, A., and Salas, M. (1992) *Gene 112*, 139−44.
13. Blasco, M. A., Lazaro, J. M., Bernad, A., Blanco, L., and Salas, M. (1992) *J. Biol. Chem. 267*, 19427−34.
14. Delarue, M., Poch, O., Tordo, N., Moras, D., and Argos, P. (1990) *Protein Eng. 3*, 461−7.
15. Karam, J. D., and Konigsberg, W. H. (1999) *Prog. Nucleic Acid Res. Mol. Biol.* (in press).
16. Doublie, S., Tabor, S., Long, A. M., Richardson, C. C., and Ellenberger, T. (1998) *Nature 391*, 251−8.
17. Li, Y., Korolev, S., and Waksman, G. (1998) *EMBO J. 17*, 7514−25.
18. Jung, G. H., Leavitt, M. C., Schultz, M., and Ito, J. (1990) *Biochem. Biophys. Res. Commun. 170*, 1294−300.
19. Blanco, L., Bernad, A., Blasco, M. A., and Salas, M. (1991) *Gene 100*, 27−38.
20. Dong, Q., Copeland, W. C., and Wang, T. S. (1993) *J. Biol. Chem. 268*, 24163−74.
21. Zhu, W., Leavitt, M. C., Jung, G., and Ito, J. (1994) *Biochim. Biophys. Acta 1219*, 260−6.
22. Dong, Q., and Wang, T. S. (1995) *J. Biol. Chem. 270*, 21563−70.
23. Beese, L. S., Friedman, J. M., and Steitz, T. A. (1993) *Biochemistry 32*, 14095−101.
24. Lin, T. C., Karam, G., and Konigsberg, W. H. (1994) *J. Biol. Chem. 269*, 19286−94.
25. Abdus Sattar, A. K., Lin, T. C., Jones, C., and Konigsberg, W. H. (1996) *Biochemistry 35*, 16621−9.
26. Brandis, J. W., Edwards, S. G., and Johnson, K. A. (1996) *Biochemistry 35*, 2189−200.
27. Astatke, M., Grindley, N. D., and Joyce, C. M. (1995) *J. Biol. Chem. 270*, 1945−54.
28. Li, Y., Kong, Y., Korolev, S., and Waksman, G. (1998) *Protein Sci. 7*, 1116−23.
29. Kaushik, N., Pandey, V. N., and Modak, M. J. (1996) *Biochemistry 35*, 7256−66.
30. Joyce, C. M., and Steitz, T. A. (1994) *Annu. Rev. Biochem. 63*, 777−822.
31. Brautigam, C. A., and Steitz, T. A. (1998) *Curr. Opin. Struct. Biol. 8*, 54−63.
32. Steitz, T. A., Smerdon, S. J., Jager, J., and Joyce, C. M. (1994) *Science 266*, 2022−5.
33. Steitz, T. A. (1998) *Nature 391*, 231−2.
34. Pelletier, H., Sawaya, M. R., Kumar, A., Wilson, S. H., and Kraut, J. (1994) *Science 264*, 1891−903.
35. Davies, J. F., II, Almassy, R. J., Hostomska, Z., Ferre, R. A., and Hostomsky, Z. (1994) *Cell 76*, 1123−33.
36. Carroll, S. S., Cowart, M., and Benkovic, S. J. (1991) *Biochemistry 30*, 804−13.
37. Bell, J. B., Eckert, K. A., Joyce, C. M., and Kunkel, T. A. (1997) *J. Biol. Chem. 272*, 7345−51.
38. Ahn, J., Werneburg, B. G., and Tsai, M. D. (1997) *Biochemistry 36*, 1100−7.
39. Saturno, J., Lazaro, J. M., Esteban, F. J., Blanco, L., and Salas, M. (1997) *J. Mol. Biol. 269*, 313−25.
40. Wang, T. S. (1991) *Annu. Rev. Biochem. 60*, 513−52.
41. Hopfner, K.-P., Eichinger, A., and Angerer B. (1999) *Proc. Natl. Acad. Sci. U.S.A. 96*, 3600−5.

BI990653W